

Document downloaded from:

<http://hdl.handle.net/10251/162586>

This paper must be cited as:

Ultimo, A.; De La Torre-Paredes, C.; Giménez, C.; Aznar, E.; Coll, C.; Marcos Martínez, MD.; Murguía, JR.... (2020). Nanoparticle-cell-nanoparticle communication by stigmergy to enhance poly(I:C) induced apoptosis in cancer cells. *Chemical Communications*. 56(53):7273-7276. <https://doi.org/10.1039/d0cc02795b>



The final publication is available at

<https://doi.org/10.1039/d0cc02795b>

Copyright The Royal Society of Chemistry

Additional Information

## Nanoparticle-cell-nanoparticle communication by stigmergy to enhance poly(I:C) induced apoptosis in cancer cells

Received 00th January 20xx,  
Accepted 00th January 20xx

Amelia Ultimo,<sup>a</sup> Cristina de la Torre,<sup>a</sup> Cristina Giménez,<sup>a</sup> Elena Aznar,<sup>a,b</sup> Carmen Coll,<sup>a,b</sup> M. Dolores Marcos,<sup>a,b,c</sup> José R. Murguía,<sup>a,b</sup> Ramón Martínez-Máñez<sup>\*a,b,c</sup> and Félix Sancenón<sup>a,b,c</sup>

DOI: 10.1039/x0xx00000x

www.rsc.org/

**Nanoparticle-cell-nanoparticle communication by stigmergy was demonstrated using two capped nanodevices. The first of nanoparticles (i.e. S(RA)<sub>IFN</sub>) is loaded with 9-cis-retinoic acid and capped with interferon- $\gamma$ , whereas the second community of nanoparticles (i.e. S(sulf)<sub>PIC</sub>) is loaded with sulforhodamine B and capped with poly(I:C). The uptake of S(RA)<sub>IFN</sub> by SK-BR-3 breast cancer cells enhanced the expression of TLR3 receptor facilitating the subsequent uptake of S(sulf)<sub>PIC</sub> and cell killing.**

Despite the progress made in nanotechnology,<sup>1</sup> there are still many challenges to be solved and there is a long way ahead in research and development before we realize its full potential. In particular, communication or cooperative behaviours at the nanoscale between nanodevices remains an almost unexplored topic. While new nanodevices are reported every year, communication and cooperation between them may expand the capabilities of single nanoparticles by allowing them to share information and to cooperate.<sup>2</sup>

Chemical or molecular communication, based on transmitting and receiving information sharing molecules (chemical messengers), is essential at cellular level and represents one of the communication forms used by living organisms. Moreover, it has been demonstrated that molecular communication can also be established in communities of nanoparticles.<sup>3</sup> In contrast to interaction mediated by direct interchange of chemical messengers, there are many examples in the nature where swarm systems communicate and cooperate by modifying the environment. This concept is called stigmergy.<sup>4</sup> However, its full power remains underappreciated and examples using nanoparticles

remains almost unexplored.

In order to explore this stigmergy concept in cell-nanoparticle communities it can be envisioned a first nanodevice acting as an allosteric activator, which is able to increase the cell ability to interact with a second wave of nanoparticles. In such mechanism, there is nanoparticle-cell-nanoparticle communication through stigmergy; despite there is not communication through chemical messengers (therefore there is not mutual “awareness”) between the two communities of nanoparticles, they are able to act cooperatively (therefore communicate), overall developing a self-organizing activity.

As a proof of concept, we describe here the use of gated nanoparticles as promising nanostructures to chemically design cooperation/communication networks.<sup>5,6</sup> Gated materials are nanoscopic devices in which the release of molecules, biomolecules or nano-objects from a porous matrix can be triggered by a target external stimulus.<sup>7</sup> In the last few years gated nano-containers, most of them based in the use of mesoporous silica nanoparticles (MSNs), have proved to be excellent candidates for the design of nanomachines at different levels and for different applications.<sup>8-13</sup>

Part of our approach is based in the use of polyinosinic-polycytidylic acid (poly(I:C)), a synthetic dsRNA agonist of TLR3 that is known to induce direct inhibition of tumour growth in different cancer cell models. Currently, several ligands for TLR3 are being evaluated in different clinical trials. A general consequence of TLR3-ligands interactions is an intense inflammatory response. Moreover, the induction of apoptotic mechanisms has also been observed in several cancers, through extrinsic pathways that lead to the final activation of effector caspases like caspase 3.<sup>14,15</sup> Hence, targeting TLR3 receptor is an effective strategy to treat different malignancies expressing TLR3.

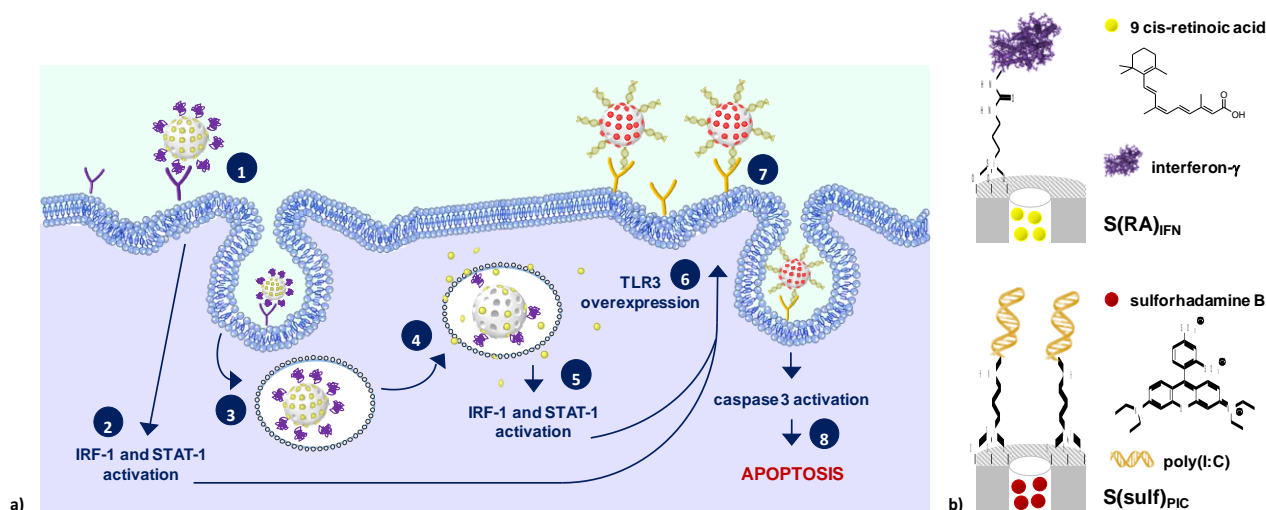
Another concept we have used is the use of 9-cis-retinoic acid (RA) and interferon- $\gamma$  (IFN) which are molecules known to induce the expression of TLR3 receptor in different studies.<sup>14,16-20</sup>

<sup>a</sup>Instituto Interuniversitario de Investigación de Reconocimiento Molecular y Desarrollo Tecnológico (IDM), Universitat Politècnica de València-Universitat de València. E-mail: rmaez@qim.upv.es

<sup>b</sup>CIBER de Bioingeniería, Biomateriales y Nanomedicina (CIBER-BBN).

<sup>c</sup>Departamento de Química, Universitat Politècnica de València, Camino de Vera s/n 46022, Valencia (Spain).

†Electronic Supplementary Information (ESI) available: Synthesis and characterization of the prepared nanoparticles, delivery studies, viability assays and confocal microscopy images. See DOI: 10.1039/x0xx00000x



**Scheme 1.** a) The mechanism of action of the cooperative nanosystems. 1.  $S(RA)_{IFN}$  nanoparticles interact with IFN receptor on the cell membrane; 2. IFN signalling activates IRF-1 and STAT-1 transcription factors; 3.  $S(RA)_{IFN}$  nanoparticles are endocytosed; 4. IFN capping moieties on  $S(RA)_{IFN}$  nanoparticles surface are degraded by lysosomal enzymes, allowing the release of RA from the mesopores; 5. RA signalling also activates IRF-1 and STAT-1; 6. TLR3 expression is induced; 7. enhanced interaction of  $S(sulf)_{PIC}$  nanoparticles with TLR3; 8. TLR3 activates extrinsic apoptotic pathways that lead to cell death. b) A schematic representation of  $S(RA)_{IFN}$  and  $S(sulf)_{PIC}$  nanoparticles.

The stigmergy cooperation protocol is based on the use of two sets of capped MSNs. The first community of MSNs ( $S(RA)_{IFN}$ ) is loaded with 9-cis-retinoic acid and capped with an interferon- $\gamma$  derivative, whereas in the second community ( $S(sulf)_{PIC}$ ) the payload is sulforhodamine B and the nanoparticles are capped with poly(l:C) (Scheme 1b). The cooperative behaviour of the two sets of nanoparticles is tested using SK-BR-3 cancer cells. The interaction of the capping interferon- $\gamma$  on  $S(RA)_{IFN}$  with its receptor located in the membrane of SK-BR-3 cells, induces both an upregulation of TLR3 expression and the internalization of the nanoparticles. Consequently, the release of 9-cis-retinoic acid due to the degradation of the gating ensemble by the lysosomal enzymes takes place. The released molecules are also expected to induce a marked enhancement in TLR3 expression in SK-BR-3 cells. Poly(l:C) in the second set of nanoparticles is known to strongly interact with TLR3, and this is expected to have a cytotoxic effect as consequence of the activation of apoptotic signalling pathways. In this combination the first community of nanoparticles performs an action (induction of TLR3 expression) and the trace of this action (a larger number of TLR3 receptors) stimulates the performance of the second community of nanoparticles (Scheme 1a).

MSNs were prepared using well-known procedures. The pores of the calcined MSNs were loaded with 9-cis-retinoic acid and the external surface functionalized with propylisocyanate moieties (solid  $S(RA)_{NCO}$ ). Then, interferon- $\gamma$  was attached onto the external surface of  $S(RA)_{NCO}$ , by means

of the formation of urea bonds, yielding the final nanoparticles  $S(RA)_{IFN}$ . In order to test the gating mechanism, similar nanoparticles but loaded with sulforhodamine B were also prepared ( $S(sulf)_{IFN}$ ). For the preparation of the second community of nanoparticles, MSNs were loaded with sulforhodamine B and the external surface decorated with aminopropyl moieties ( $S(sulf)_{NH_2}$ ). Finally, the pores were capped upon reaction of the activated phosphate groups of poly(l:C) with the aminopropyl moieties grafted onto the external surface yielding  $S(sulf)_{PIC}$ . The prepared nanoparticles were characterized using standard procedures (see Supporting Information for details). Moreover, sulforhodamine B release from  $S(sulf)_{IFN}$  and  $S(sulf)_{PIC}$  in the presence of lysosomal extract was tested (Figure 1). As can be seen, sulforhodamine B release from solid  $S(sulf)_{IFN}$  and  $S(sulf)_{PIC}$  was low in the absence of the extract (release < 15 % of maximum release after 25 h), which indicates the correct capping of the material by the bulky interferon- $\gamma$  (in  $S(sulf)_{IFN}$ ) and poly(l:C) (in  $S(sulf)_{PIC}$ ). In contrast, a remarkable cargo release occurred for both solids in the presence of lysosomal extract. This is attributed to enzymatic degradation of the interferon- $\gamma$  and poly(l:C) caps, which induced sulforhodamine B release. Besides it was confirmed that selected interferents ( $Na^+$ ,  $K^+$ ,  $Ca^{2+}$ ,  $Fe^{3+}$ , Cys, GSH,  $H_2O_2$ ) or changes in the pH (4, 7 and 9) did not induce sulforhodamine B release from  $S(sulf)_{IFN}$  and  $S(sulf)_{PIC}$  nanoparticles (Figure S1-3).

Cell viability assays with both  $S(RA)_{IFN}$  and  $S(sulf)_{PIC}$  solids were carried out. The underlying idea was to compare the

cytotoxic effect exerted by poly(I:C) in SK-BR-3 cells using **S(sulf)<sub>PIC</sub>** nanoparticles alone or in combination with a pre-treatment with **S(RA)<sub>IFN</sub>**. Besides, in order to highlight the cooperation between nanoparticles, viability assays with free poly(I:C) and poly(I:C) combined with free 9-cis-retinoic acid and interferon- $\gamma$ , at the same concentrations as in the nanoparticles, were also carried out. The obtained results are presented in Figure 2a that shows dose-response curves after 48 h experiments carried out with **S(sulf)<sub>PIC</sub>** alone (using the required amounts of nanoparticles to reach a poly(I:C) concentration in the 0.001-500  $\mu\text{g mL}^{-1}$  range) or treatment with **S(sulf)<sub>PIC</sub>** after 4 h pre-treatment with **S(RA)<sub>IFN</sub>** solid. For **S(RA)<sub>IFN</sub>** it was used the appropriate quantity of nanoparticles to obtain a 9-cis-retinoic acid concentration of 0.3  $\mu\text{g mL}^{-1}$ . Moreover, Figure 2a also shows the curves obtained when cells are treated with poly(I:C) alone or treated with poly(I:C) after 4 h pre-treatment of the cells with 9-cis-retinoic acid (0.3  $\mu\text{g mL}^{-1}$ ) and interferon- $\gamma$  (15  $\text{ng mL}^{-1}$ ). As shown in Figure 2a, free poly(I:C) cytotoxicity on SK-BR-3 cells is negligible at the tested concentrations, while it is only slightly enhanced after pre-treatment with free 9-cis-retinoic acid and interferon- $\gamma$ , pointing out the importance of the nanoformulation when data is compared with the treatment using **S(sulf)<sub>PIC</sub>** or **S(RA)<sub>IFN</sub>** + **S(sulf)<sub>PIC</sub>** combination (*vide infra*).

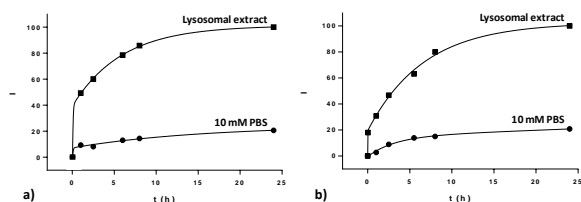


**Figure 1.** Cargo delivery profiles from solids (a) **S(sulf)<sub>IFN</sub>** and (b) **S(sulf)<sub>PIC</sub>**, in the absence and in the presence of lysosomal extract.

To confirm the TLR3-mediated **S(sulf)<sub>PIC</sub>** nanoparticles internalization confocal microscopy measurements were carried out. SK-BR-3 cell cultures were treated for 48 h with **S(sulf)<sub>PIC</sub>** (50  $\mu\text{g mL}^{-1}$  of equivalent poly(I:C)). A clear sulforhodamine B fluorescence was observed in the cytosol of SK-BR-3 cells treated with **S(sulf)<sub>PIC</sub>**, indicating internalization of nanoparticles and subsequent uncapping and dye release in the lysosomes (Figure 3).

Most interestingly, when SK-BR-3 cells were pre-treated with **S(RA)<sub>IFN</sub>** and then incubated with **S(sulf)<sub>PIC</sub>**, a remarkable decrease in cells viability, when compared to that obtained when using **S(sulf)<sub>PIC</sub>** alone, was observed. For example, at 25  $\mu\text{g mL}^{-1}$  poly(I:C) concentration, cell viability was reduced from 90% to 65% when treated with **S(sulf)<sub>PIC</sub>** alone or with both **S(RA)<sub>IFN</sub>**+**S(sulf)<sub>PIC</sub>** nanoparticles, respectively. Overall **S(RA)<sub>IFN</sub>** and **S(sulf)<sub>PIC</sub>** nanoparticles act cooperatively by stigmergy. The first community of nanoparticles (i.e. **S(RA)<sub>IFN</sub>**) perform an action (delivery of interferon- $\gamma$  and 9-cis-retinoic that act as chemical cues that enhance the overexpression of membrane TLR3 receptors) and the trace of this action (enhanced expression of TLR3 receptors) stimulates the performance of the second community of nanoparticles (i.e. **S(sulf)<sub>PIC</sub>**) that are more effectively internalized and enhanced cell killing. This was confirmed by Western blot

assays (Figure 2b) that demonstrated the induction of TLR3 expression in SK-BR-3 cells by **S(RA)<sub>IFN</sub>** nanoparticles.

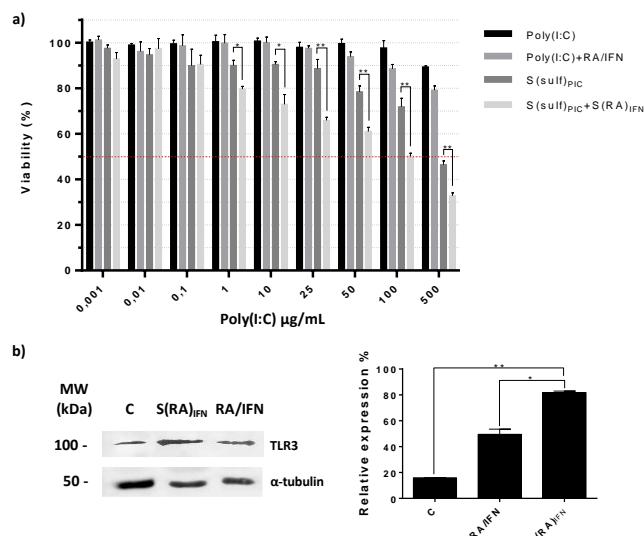


**Figure 2.** (a) Dose-response curves after 48 h for cells treated with free poly(I:C), with 9-cis-retinoic acid and interferon- $\gamma$  for 4 h and then with poly(I:C), with **S(sulf)<sub>PIC</sub>** and, finally, with **S(RA)<sub>IFN</sub>** for 4 h and then with **S(sulf)<sub>PIC</sub>**. Cell viability was determined by using the cell proliferation reagent WST-1. Concentrations between 0.001 and 500  $\mu\text{g mL}^{-1}$  of free poly(I:C) and equivalent poly(I:C) in **S(sulf)<sub>PIC</sub>** were tested. 15  $\text{ng mL}^{-1}$  of interferon- $\gamma$  and 0.3  $\mu\text{g mL}^{-1}$  of 9-cis-retinoic acid and equivalent 9-cis-retinoic acid in **S(RA)<sub>IFN</sub>** were used. All values are shown as the mean  $\pm$  SD ( $n=3$ ). Asterisks indicate significant differences (\* =  $p < 0.01$ , \*\* =  $p < 0.001$ ) when t test was applied. (b) Representative immunoblots showing induction of TLR3 in SK-BR-3 cells after a 24 h treatment with free 9-cis-retinoic acid (0.3  $\mu\text{g mL}^{-1}$ ) and interferon- $\gamma$  (15  $\text{ng mL}^{-1}$ ) or with **S(RA)<sub>IFN</sub>**. Relative expression of TLR3 was calculated by densitometry, normalizing by the loading control ( $\alpha$ -Tubulin). Expression values are shown as the mean  $\pm$  SD ( $n=3$ ). Asterisks indicate significant differences (\* =  $p < 0.001$ , \*\* =  $p < 0.0001$ ) when t test was applied.

We also carried out additional viability experiments using flow cytometry at an equivalent concentration of poly(I:C) of 500  $\mu\text{g mL}^{-1}$ . In this experiment, a well-known inhibitor of TLR3 receptor ((*R*)-2-(3-chloro-6-fluorobenzo[*b*]thiophene-2-carboxamido)-3-phenylpropanoic acid)<sup>21</sup> was also used. Similar results to those obtained in Figure 2a for the same poly(I:C) concentration were found (Figure 4). Thus, the viability of SK-BR-3 cells treated with poly(I:C), interferon- $\gamma$  + 9-cis-retinoic acid and poly(I:C) + interferon- $\gamma$  + 9-cis-retinoic remained virtually unchanged. A moderate reduction to ca. 55% viability was observed when SK-BR-3 cells were treated with a mixture of interferon- $\gamma$  and 9-cis-retinoic and then administered with **S(sulf)<sub>PIC</sub>** or with the nanoparticles alone (viability ca. 60%). However, when cells were treated with TLR3 inhibitor and **S(sulf)<sub>PIC</sub>**, cell viability increased to ca. 80%. This enhancement in viability is consistent with the blockage of TLR3 receptor by the inhibitor and, as a consequence, the reduced uptake of **S(sulf)<sub>PIC</sub>** nanoparticles. Besides, in these flow cytometry studies a marked reduction in SK-BR-3 cells viability (to ca. 20%) was observed when both nanoparticles were administered sequentially, thus reinforcing the stigmergy protocol of the nanodevices community.



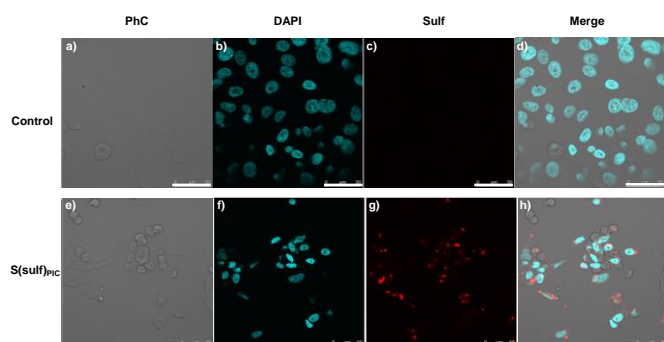


**Figure 3.** Internalization and release of sulforhodamine B (red) in SK-BR-3 cells. Cultures were incubated with **S(sulf)<sub>PIC</sub>** for 48 h and examined by confocal microscopy. Cells nuclei were stained with DAPI (blue) before microscope observation. Representative images for phase contrast (PhC, a, e), DAPI (b, f), sulforhodamine B (sulf, c, g) and combined (merge, d, h) are shown. Scale bar = 50  $\mu\text{m}$ .

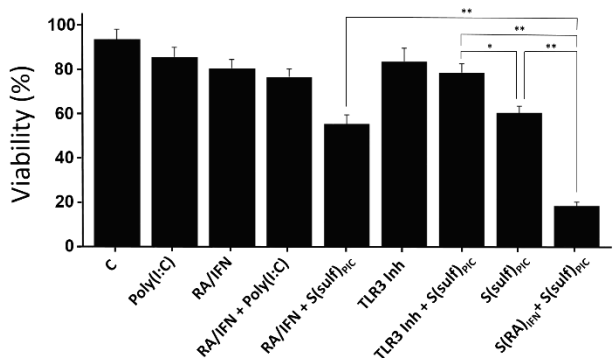


**Figure 4.** Analysis of cell viability by flow cytometry. A concentrations of 500  $\mu\text{g mL}^{-1}$  of free poly(I:C) and equivalent poly(I:C) in **S(sulf)<sub>PIC</sub>** was tested. 15  $\text{ng mL}^{-1}$  of interferon- $\gamma$  and 0.3  $\mu\text{g mL}^{-1}$  of 9-cis-retinoic acid and equivalent 9-cis-retinoic acid in **S(RA)<sub>IFN</sub>** were used. Data represents the mean  $\pm$  SD ( $n=3$ ). Asterisks indicate significant differences (\* =  $p < 0.001$ , \*\* =  $p < 0.0001$ ) when t test was applied.

In summary, we present here a proof of concept of a nanoparticle-cell-nanoparticle communication model involving two nanodevices. The first set of nanoparticles are loaded with 9-cis-retinoic acid and capped with interferon- $\gamma$  (**S(RA)<sub>IFN</sub>**), whereas in the second nanodevice sulforhodamine B was used as cargo and poly(I:C) chains as caps (**S(sulf)<sub>PIC</sub>**). The uptake of **S(RA)<sub>IFN</sub>** by SK-BR-3 breast cancer cells enhanced the overexpression of TLR3 receptor that facilitated the subsequent internalization of **S(sulf)<sub>PIC</sub>**. As a consequence, a marked reduction in cells viability was observed when both communities of nanoparticles were used in a combined treatment, compared to that obtained with **S(sulf)<sub>PIC</sub>** alone or by a combination of free 9-cis-retinoic, interferon- $\gamma$  and poly(I:C). The results presented in this work demonstrate the possibility of developing stigmergy communication/cooperation strategies involving communities of nanodevices and cells. Such stigmergy protocols may enhance nanocarrier outcomes and potentiate their applications in targeted transport and drug delivery, opening wide new scenarios of cooperation/communication between nanoparticles and leading to the design of a number of

plausible networks with the aim to increase drug efficacy and to reduce dosages, side effects, and resistance.

We thank the Spanish Government (projects RTI2018-100910-B-C41 and RTI2018-101599-B-C22 (MCUI/FEDER, EU)) and the Generalitat Valenciana (project PROMETEO2018/024) for support. A.U. is grateful to the Ministry of Education, Culture and Sport for her doctoral FPU grant.

### Conflicts of interest

There are no conflicts to declare.

### References

- D. Schaming and H. Remita, *Found. Chem.*, 2015, **17**, 187.
- S. Hauert and S. N. Bhatia, *Trends Biotechnol.*, 2014, **32**, 448.
- T. Nakano, M. J. Moore, F. Wei, A. V. Vasilakos and J. Shuai, *IEEE Trans. Nanobiosci.*, 2012, **11**, 135.
- G. Theraulaz and E. Bonabeau, *Artif. Life* 1999, **5**, 97-116.
- C. Giménez, E. Climent, E. Aznar, R. Martínez-Mañez, F. Sancenón, M. D. Marcos, P. Amorós and K. Rurack, *Angew. Chem. Int. Ed. Engl.*, 2014, **53**, 12629.
- a) A. Llopis-Lorente, P. Díez, A. Sánchez, M. D. Marcos, F. Sancenón, P. Martínez-Ruiz, R. Villalonga and R. Martínez-Mañez, *Nat. Commun.*, 2017, **30**, 15511; b) B. de Luis, A. Llopis-Lorente, P. Rincln, J. Gadea, F. Sancenón, E. Aznar, R. Villalonga, J.R. Murguía, R. Martínez-Mañez, *Angew. Chem. Int. Ed.* 2019, **58**, 14986
- E. Aznar, M. Oroval, L. Pascual, J. R. Murguía, R. Martínez-Mañez and F. Sancenón, *Chem. Rev.*, 2016, **116**, 561
- C. de la Torre, L. Domínguez-Berrocal, J. R. Murguía, M. D. Marcos, R. Martínez-Mañez, J. Bravo and F. Sancenón, *Chem. Eur. J.*, 2018, **24**, 1890.
- A. García-Fernández, G. García-Laínez, M. L. Ferrándiz, E. Aznar, F. Sancenón, M. J. Alcaraz, J. R. Murguía, M. D. Marcos, R. Martínez-Mañez, A. M. Costero and Mar Orzáez, *J. Control. Release*, 2017, **248**, 60.
- C. Yu, L. Qian, M. Uttamchandani, L. Li and S. Q. Yao, *Angew. Chem. Int. Ed.*, 2015, **54**, 10574.
- C. Murugan, K. Rayappa, R. Thangam, R. Bhanumathi, K. Shanthi, R. Vivek, R. Thirumurugan, A. Bhattacharyya, S. Sivasubramanian, P. Gunasekaran and S. Kannan, *Sci. Rep.*, 2016, **6**, 34053.
- S. H. van Rijt, D. A. Bölükbas, C. Argyo, S. Datz, M. Lindner, O. Eickelberg, M. Königshoff, T. Bein and S. Meiners, *ACS Nano*, 2015 **9**, 2377.
- A. Llopis-Lorente, B. Lozano-Torres, A. Bernardos, R. Martínez-Mañez and F. Sancenón, *J. Mater. Chem. B*, 2017, **5**, 3069.
- F. Bianchi, S. Pretto, E. Tagliabue, A. Balsaria and L. Sfondrini, *Cancer Biol. Ther.*, 2017, **18**, 747.
- A. Ultimo, C. Giménez, P. Bartovsky, E. Aznar, F. Sancenón, M. D. Marcos, P. Amorós, A. R. Bernardo, R. Martínez-Mañez, A. M. Jiménez-Lara and J. R. Murguía, *Chem. Eur J.*, 2016, **22**, 1582.
- A. R. Bernardo, J. M. Cosgaya, A. Aranda and A. M. Jiménez-Lara, *Cell Death Dis.*, 2013, **4**, e479.
- N. Clarke, A. M. Jiménez-Lara, E. Voltz and H. Gronemeyer, *EMBO J.*, 2004, **23**, 3051.
- A. Kajita, S. Morizane, T. Takiguchi, T. Yamamoto, M. Yamada and K. Iwatsuki, *J. Invest. Dermatol.*, 2015, **135**, 2005.
- C. M. Horvat, *Sci. STKE*, 2004, **2004**, tr8.
- X. Weihua, V. Kolla and D. V. Kalvakolanu, *J. Biol. Chem.*, 1997, **272**, 9742.
- K. Cheng, X. Wang and H. Yin, *Chem. Commun.*, 2011, **133**, 3764.